PERGAMON

Journal of Structural Geology 22 (2000) 81–89

JOURNAL OF STRUCTURAL GEOLOGY

www.elsevier.nl/locate/jstrugeo

Misorientations across etched boundaries in deformed rocksalt: a study using electron backscatter diffraction

Patrick W. Trimby*, Martyn R. Drury, Christopher J. Spiers

Geodynamics Research Institute, Faculty of Earth Sciences, Utrecht University, PO Box 80.021, 3508 TA Utrecht, The Netherlands

Received 10 March 1999; accepted 25 June 1999

Abstract

Automated electron backscatter diffraction (EBSD) in the scanning electron microscope has been used to collect crystallographic orientation and misorientation data from etched surfaces of deformed synthetic rocksalt. By comparing the misorientation across individual boundaries to the intensity of etching, we have assessed the effectiveness of the etching procedure. High angle ($>10^{\circ}$) grain boundaries are typically etched significantly more than low angle subgrain boundaries, and thus they can be easily identified using reflected light microscopy. However, there exists considerable variation in the intensity of etching of subgrain boundaries, independent of their misorientation. The intensity of intragranular boundary etching is controlled by the crystallographic orientation of the etched surface: surfaces close to {100} faces are only lightly etched, while surfaces close to {111} faces are heavily etched. Therefore, whilst reflected light microscopy of etched surfaces of deformed rocksalt remains extremely useful for general microstructural characterisation, fully quantitative techniques such as EBSD are ideal for more detailed microstructural analyses. © 1999 Elsevier Science Ltd. All rights reserved.

1. Introduction

Rocksalt is a material of great geological importance. This is due to its role in a variety of tectonic processes, in hydrocarbon trapping phenomena and its use as a disposal and storage medium (e.g. Janssen et al., 1984; Spiers et al., 1989; Duval et al., 1992; Carter et al., 1993; Weijermans et al., 1993). Such economic and scientific interest has resulted in many detailed studies of its properties, especially its long-term rheological and transport properties (e.g. Heard, 1972; Sutherland and Cave, 1980; Carter and Hansen, 1983; Urai et al., 1986; Wawersik and Zeuch, 1986; Spiers et al., 1990; Carter et al., 1993; Peach and Spiers, 1996). The similarities between the microstructural processes observed in deformed rocksalt and those operating in silicate rocks at high pressures and temperatures have also made rocksalt a useful analogue material for understanding microstructural processes (e.g. Guillopé and Poirier, 1979; Drury and Urai, 1990) and the development of lattice preferred orientations in rocks in general (Wenk et al., 1989, 1997). However, halite is a cubic mineral, and hence optically isotropic. This largely rules out investigation of halite microstructures and crystallographic orientations using polarised light microscopy, although limited information can be gained from studies of deformation-induced birefrigence (Carter and Hansen, 1983). Instead, grain and subgrain boundaries are usually revealed by polishing and/or etching procedures coupled with reflected light examination (e.g. Mendelson, 1961; Guillopé and Poirier, 1979; Carter and Hansen, 1983; Urai et al., 1987). More recently, gamma-irradiation techniques have been used to decorate subgrain boundaries and other dislocation substructures with metallic sodium, thereby rendering them visible in transmitted light (Urai et al., 1987; Spiers and Carter, 1998). While both etching and irradiation have proved to be valuable techniques, the assessment of misorientations across boundaries based on the intensity of etching or of decoration is qualitative and uncalibrated. There exist a number of techniques which have been used to

* Corresponding author.
E-mail address: trimby@geo.uu.nl (P.W. Trimby)

0191-8141/00/$ - see front matter © 1999 Elsevier Science Ltd. All rights reserved.
PII: S0191-8141(99)00126-1

calculate the crystallographic orientations of grains and the misorientations across boundaries in deformed rocksalt. These include the use of cubic surface textures (Friedman et al., 1984), measuring the orientation of {100} cleavage planes bounding intragranular fluid inclusions (Friedman et al., 1984), producing epitaxial overgrowths of fine NaCl crystallites on etched surfaces (Urai et al., 1987) and a variety of Laue and Kossel X-ray techniques (e.g. Guillopé and Poirier, 1979). However, such techniques are either limited by microstructural considerations (such as grain size), or by practical difficulties which exacerbate the collection of accurate and representative data.

Electron backscatter diffraction (EBSD) in the scanning electron microscope (SEM) allows the orientations of crystal lattices from sub-micron areas to be determined (e.g. Venables and Harland, 1972; Dingley, 1984). It has been widely applied in materials science (e.g. Dingley and Randle, 1992; Field, 1995; Goyal et al., 1997) but only recently to the earth sciences (e.g. Trimby et al., 1998; Faul and Fitz Gerald, 1999; Fliervoet et al., 1999; Trimby and Prior, 1999). Until now, EBSD has not been successfully applied to rocksalt, as far as we are aware. This is because rocksalt undergoes rapid radiation damage when subjected to a high energy electron beam, resulting in very poor quality electron backscatter patterns (EBSPs). However, recent advances in computing software and hardware capabilities, coupled with the use of a field emission gun (FEG) SEM, allow good quality EBSPs to be collected and indexed before significant sample damage is incurred. Thus we can now use EBSD to analyse the crystallographic nature of inter- and intra-granular boundaries in deformed rocksalt. In this paper we use EBSD data to evaluate the misorientations across etched boundaries, and to assess objectively the effectiveness of the etching procedure in revealing the microstructure of rocksalt.

2. Techniques

Two contrasting samples were used to investigate the misorientations across etched boundaries. Synthetic rocksalt with a starting grain size of 200–450 μm was experimentally deformed in a triaxial deformation apparatus (Peach, 1991; Peach and Spiers, 1996) at strain rates of $\sim 5.5 \times 10^{-7}\ s^{-1}$ and at a confining pressure of 50 MPa. One sample, p40t92, contained sufficient water (68 ppm) to support fluid assisted dynamic recrystallisation via grain boundary migration (Urai et al., 1986; Spiers and Carter, 1998); this 'wet' salt was deformed to 18.2% strain at a temperature of 125°C. A second sample, p40t98, was effectively dry (~5 ppm water); this was deformed to 28.2% strain at $T = 175$°C. No grain boundary migration occurs under these conditions. Instead, microstructural development is dominated by intense subgrain formation, but the extent of subgrain rotation and boundary misorientation development is unknown.

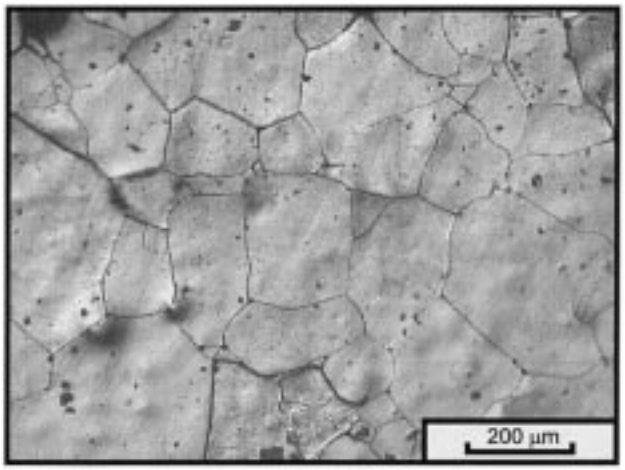

Fig. 1. Reflected light photomicrograph of the starting material for the wet salt experiments. The starting material for the dry salt experiments is very similar.

The deformed samples were cut into small blocks (~15 × 15 mm) and were polished and etched following the method described by Spiers et al. (1986) and Urai et al. (1987). This involved dry sawing, initial grinding and polishing and then a final period of simultaneous chemical polishing and etching. This last stage was done in a slightly undersaturated NaCl solution containing about 0.8 wt% $FeCl_3 \cdot 6H_2O$; the samples were immersed and gently agitated for about 10 s before the etchant was removed by alternating blasts of n-hexane and diethyl ether. Finally the samples were dried in a stream of hot air, mounted for SEM work and their edges coated with conductive silver paint.

Prior to SEM study, the etched surfaces were imaged in reflected light using a Leica DMRX microscope. The images were captured electronically and processed using Leica's Qwin Pro v2.2 software. The microstructure of the starting material for the wet salt experiment is shown in Fig. 1. This is characterised by polygonal grains, 120° triple junction grain boundaries and an almost complete absence of intra-grain microstructure. The starting material for the dry salt experiments is very similar. In each of the deformed samples, an area of interest was chosen for detailed EBSD analysis in the SEM.

The SEM analysis was carried out in a Philips XL30 FEG SEM using a 10 kV accelerating voltage and a system spot size 5 (equating to a beam current ~6.7 nA). The areas identified using reflected light microscopy were located in the SEM using a forescatter

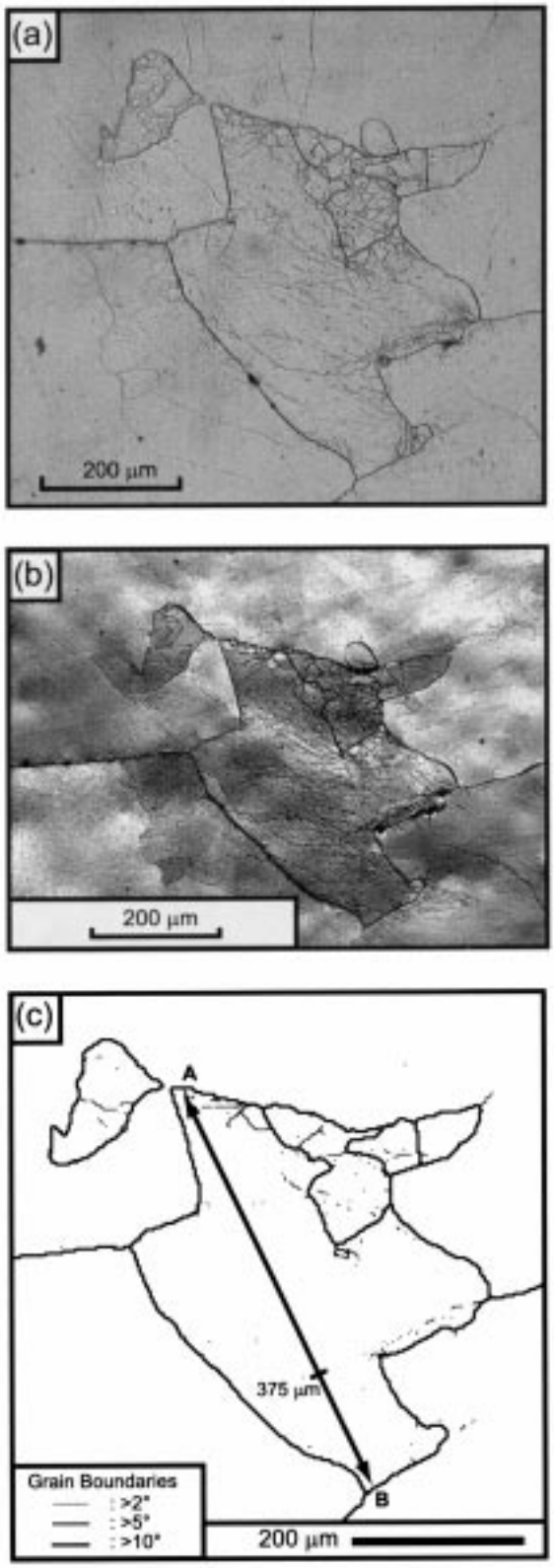

Fig. 2. (a) Reflected light photomicrograph of the wet salt sample, p40t92. (b) Orientation contrast image of the same area collected in the SEM using a forescatter detector. (c) Boundary misorientation map of the same area constructed from a 250 × 250 grid of EBSD data points taken at a 2.5 μm spacing. Line A–B marks the location of a detailed transect (see Fig. 3).

detector to provide an orientation contrast (OC) image (Prior et al., 1996).

For each area, EBSPs were collected from a grid of regularly spaced points by automatically moving the electron beam. This technique, sometimes referred to as 'orientation imaging microscopy', is commonly used in the materials sciences (e.g. Adams et al., 1993; Field, 1997). The EBSPs were indexed using the software CHANNEL+, with a halite structure file consisting of 46 lattice planes. On average, each EBSP took ~0.17 s to collect and index; this rapid processing time prevented significant surface radiation damage from occurring. EBSPs were collected from a 250 × 250 orthogonal grid (2.5 μm spacing) for sample p40t92, and from a 300 × 300 orthogonal grid (2 μm spacing) for sample p40t98. The misorientations between adjacent data points were calculated, and this information was used to display boundary misorientation maps—maps where different boundary misorientations are represented by different line thicknesses. For each misorientation, the cubic symmetry of halite results in 24 symmetrically equivalent solutions; following convention, we always took the minimum misorientation angle (e.g. Randle, 1992, 1993). The indexing error in each EBSD solution is accepted to be $<1^\circ$ (e.g. Dingley and Randle, 1992); it is possible, using double exposure of diffraction patterns from adjacent areas separated by a low angle boundary, to measure accurately very small ($\ll 1^\circ$) misorientations (Hutchinson, Hall and Lloyd, unpublished work, 1979). This technique is ideal for the study of individual boundaries but it has not been utilised here. Therefore, in this study, the error in the calculated misorientation angle between two grains in the same sample will be in the range 0–2° and for this reason boundaries with misorientations $<2^\circ$ have not been displayed on the boundary misorientation maps. The manipulation of the raw data was carried out using the software CHANNEL+ICE, and maps with boundary misorientation intervals of 2–5°, 5–10° and $>10^\circ$ have been generated. These maps were then compared with the reflected light photomicrographs in order to evaluate the etching procedure and to assess the relative merits of both techniques.

3. Results

3.1. Sample p40t92

The reflected light photomicrograph of the wet sample (p40t92) is shown in Fig. 2(a). The microstructure here is characterised by several relatively small grains in the centre, with considerable substructure, surrounded by three large grains with little or no substructure. In comparison with the starting material

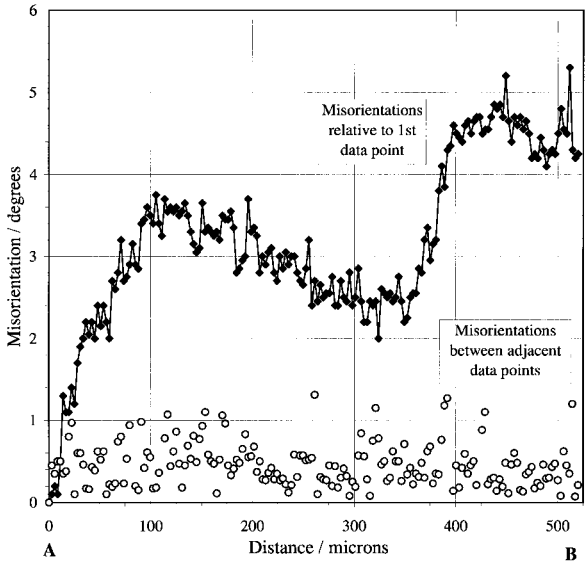

Fig. 3. Graph showing the misorientation variations along the transect A–B (see Fig. 2c). The upper line (black diamonds) represents the cumulative misorientation with respect to the first data point at A. The open circles represent the misorientations between adjacent points.

microstructure (Fig. 1), it is apparent that there has been a significant increase in grain size of the larger grains, and the development of considerable substructure in some of the smaller grains. With grain boundary migration clearly the dominant recrystallisation process in this sample, the small grains are interpreted as older grains that have been partially consumed by the large, new, substructure-poor grains. The sub-parallel wavy lines apparent in the upper and lower left parts of the image are inferred to indicate combined slip and cross-slip of screw dislocations (Senseny et al., 1992; Carter et al., 1993; Spiers and Carter, 1998). The more irregular etched lines inside the older grains are interpreted as being low angle subgrain boundaries (e.g. Urai et al., 1987); in places these form cellular features, whereas elsewhere they appear 'blind ending' (i.e. the boundaries terminate inside grains). The more deeply etched lines, with occasional fluid inclusions, are the high angle grain boundaries. The OC image of the same area is shown in Fig. 2(b); the etched boundaries are readily apparent, and a weak orientation contrast between different grains and subgrains is visible.

The boundary misorientation map of the same area is shown in Fig. 2(c). It is immediately apparent that the most heavily etched boundaries in the light photomicrograph do indeed correspond to high angle ($>10^\circ$) grain boundaries. The interiors of the old grains, despite having many etched boundaries, have very few boundaries with misorientations $>2^\circ$.

In order to investigate further the nature of this low angle intra-granular microstructure, a transect A–B (see Fig. 2c) was analysed in greater detail. Using the EBSD data, the misorientation of each data point along the transect relative to the orientation of the first data point (at A) was calculated. This gives the cumulative misorientation across the grain, indicating the nature and the extent of any crystal lattice orientation variations. In order to show the misorientations across individual boundaries along the transect, the misorientations between adjacent data points have also been calculated. These data are plotted against the distance along the transect in Fig. 3. This graph helps to explain the differences between Figs. 2(a) and (c). In places, such as ~375 μm from A (marked on Fig. 2c), there are relatively rapid changes in the cumulative misorientation of up to 3°. However, even these occur over a distance of ~50 μm and we also observe (Fig. 3) that the misorientations between adjacent grid points do not exceed 1.3°. These results show us two things. Firstly, the majority of the visible intra-granular boundaries in the reflected light photomicrograph (Fig. 2a) have very low misorientations, below the 2° angular resolution of the boundary misorientation map. Secondly, in two examples along this transect (and in many other grains in this sample), these very low angle boundaries add up to create more significant crystallographic orientation changes across whole grains.

3.2. Sample p40t98

The reflected light photomicrograph of the dry sample (p40t98) is shown in Fig. 4(a). In the field of view, which is approximately the same size as in Fig. 2(a), there are about 15 identifiable grains, all with varying degrees of substructure. The grain size is still similar to that of the starting material (Fig. 1), although many of the boundaries have become serrated on the scale of the cellular substructure. There is no evidence for large scale grain boundary migration. Some of the grains, such as one near the top left corner ('C'), show a heavily etched substructure while other grains, such as the one in the lower right corner ('D'), exhibit a lightly etched substructure or appear relatively substructure free. Although most of the substructure forms cellular features, some boundaries, as in Fig. 2(a), appear to be 'blind ending'. Locally (e.g. in the lower left corner), numerous heavily etched boundaries make the distinction between high angle and low angle boundaries problematical. The OC image of the same area is shown in Fig. 4(b). Although many of the etched boundaries are clearly visible, the magnitude of any orientation contrast is small. The polishing and etching procedure does not remove all of the surface topography; the high tilt angle and the position of the forescatter detector below the specimen accentuates this topography, resulting in a reduction or even the removal of any orientation contrast signal. The OC image is thus only

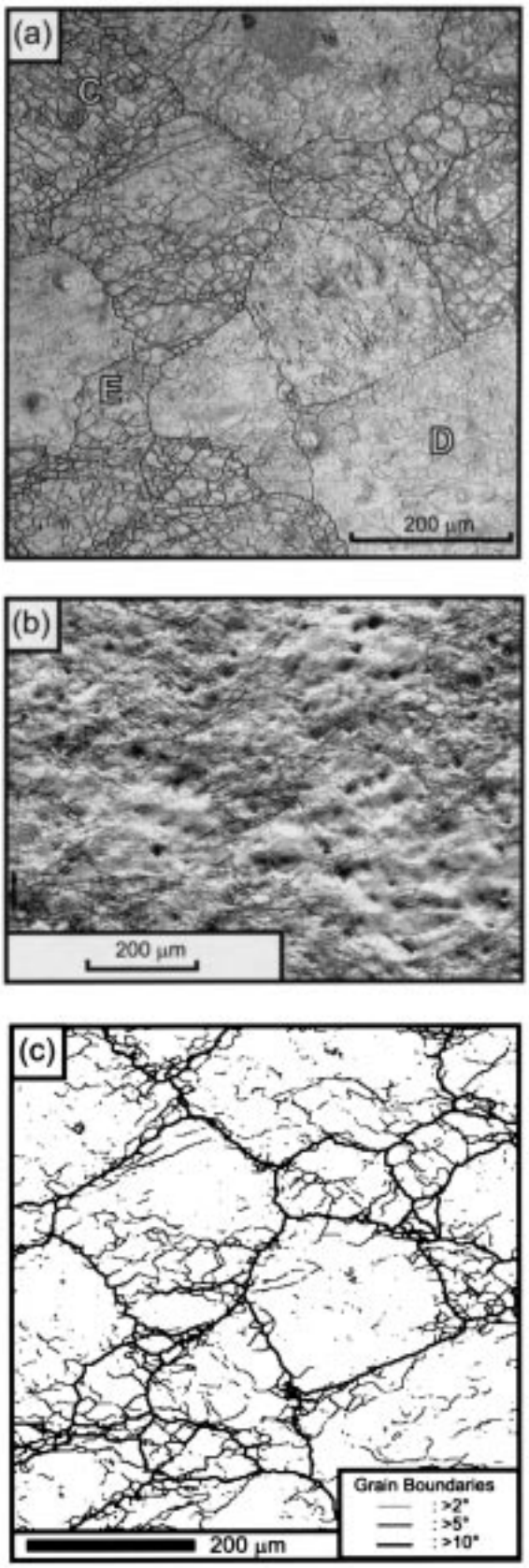

Fig. 4. (a) Reflected light photomicrograph of the dry salt sample, p40t98. Grains C, D and E are referred to in the text. (b) Orientation contrast image of the same area collected in the SEM using a forescatter detector. (c) Boundary misorientation map of the same area constructed from a 300 × 300 grid of EBSD data points taken at a 2 μm spacing.

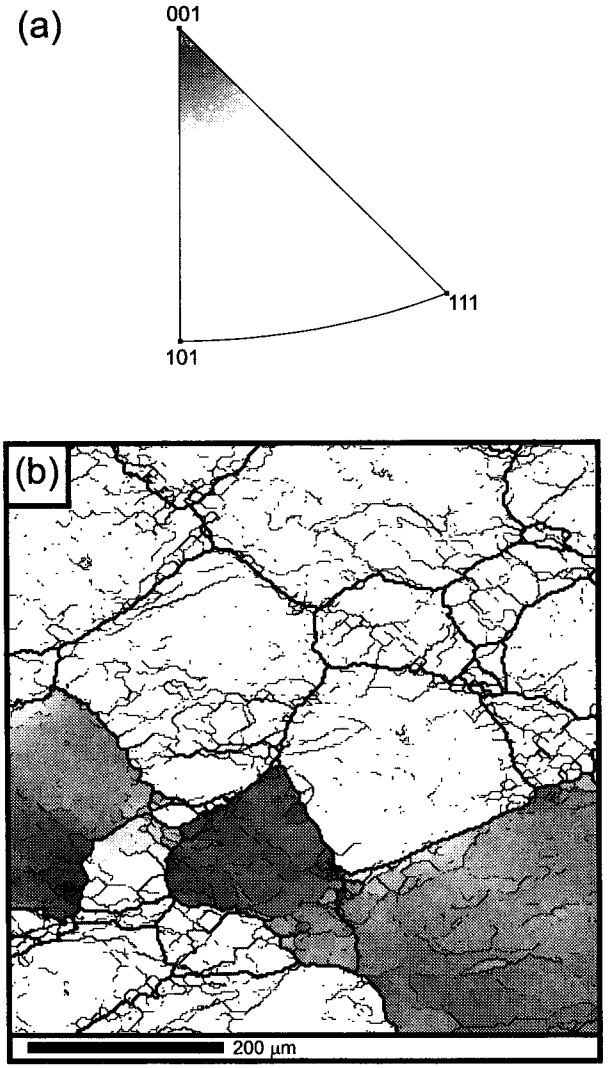

Fig. 5. (a) Inverse pole figure of the surface normals for the dry salt sample, showing only those data points with the surface normals within 15° of the ⟨001⟩ direction. Equal area projection. (b) Boundary misorientation map showing the spatial distribution of those data points featured in (a).

useful (for these samples) for identifying the area of interest prior to EBSD analysis.

The boundary misorientation map for the same area is shown in Fig. 4(c). As observed in the wet sample, most of the heavily etched boundaries do correspond to high angle grain boundaries. However the heavily etched substructures observed in many of the grains (see Fig. 4a) do not correspond to significant misorientations (>2°). For example, the misorientation map

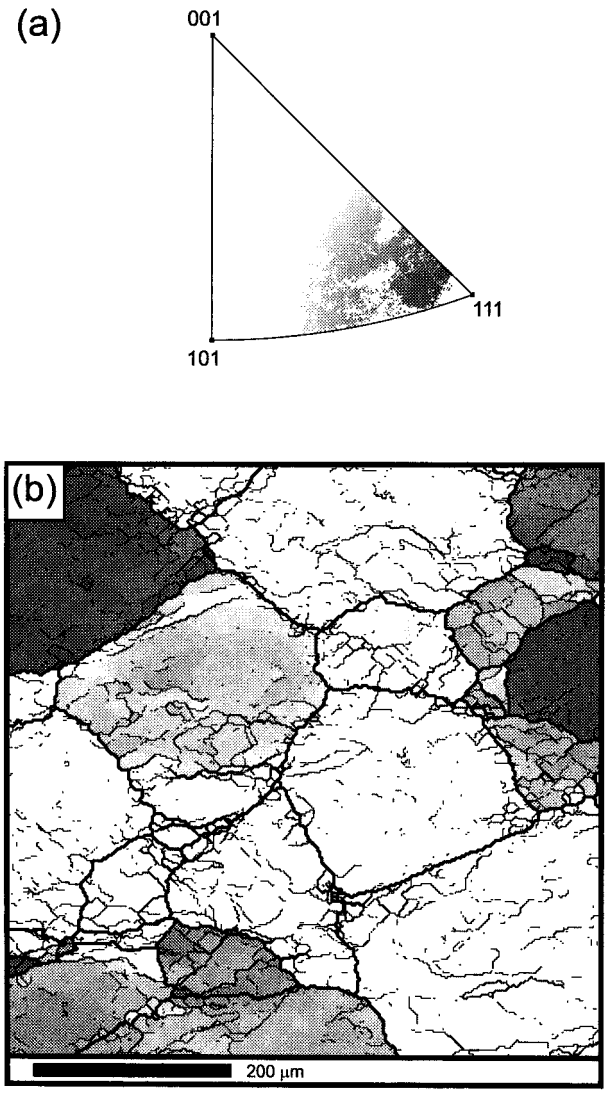

Fig. 6. (a) Inverse pole figure of the surface normals for the dry salt sample, showing only those data points with the surface normals within 25° of the ⟨111⟩ direction. Equal area projection. (b) Boundary misorientation map showing the spatial distribution of those data points featured in (a).

shows that the aforementioned grain C, although from the depth of etching it appears to have considerable substructure, does in fact contain few subgrain boundaries $>2°$, and virtually none $>5°$. In comparison, some other grains which display lighter etching (e.g. grain 'E'), actually contain subgrain boundaries with misorientations $>5°$, and even $>10°$ (i.e. some have become high angle boundaries). It is clear that there exists a range of subgrain boundary misorientations in this sample, the extent of which is not immediately apparent from the intensity of the etching.

The variations in the intensity of etching between grains with substructures of similar misorientations can be related to the grains' crystallographic orientations. In order to check whether particular crystallographic orientations result in preferential etching, we have plotted the surface normal directions on inverse pole figures. Grains with the surface normal close to the ⟨001⟩ direction must have a {100} face almost parallel to the surface of the sample. Likewise, those with the ⟨111⟩ direction close to the surface normal will have a {111} face almost parallel to the sample surface. In Fig. 5(a) all the data points where the surface normal is within 15° of the ⟨001⟩ direction have been plotted on an inverse pole figure, and the corresponding grains shaded on a boundary misorientation map (Fig. 5b). Comparison with the reflected light photomicrograph (Fig. 4a) shows that the three grains which have been shaded also display the least etching of any grains in the whole area. Data points where the surface normal is within 25° of the ⟨111⟩ direction have also been plotted on an inverse pole figure (Fig. 6a), and shaded on an accompanying boundary misorientation map (Fig. 6b). This time, comparison with the reflected light photomicrograph (Fig. 4a) shows that all the shaded grains display relatively intense etching. In particular, the heavily etched grain discussed earlier (grain C) has a {111} face almost parallel to the surface of the sample. It is also worth noting, from Fig. 4(c), that the subgrain boundary misorientations in grain C are certainly no greater than those in grains D and E, despite being much more heavily etched.

4. Discussion and conclusions

The purpose of this paper is two-fold: firstly to introduce the application of EBSD to studies of deformed rocksalt, and secondly to attempt to relate the width and intensity of etched boundaries in rocksalt samples to their crystallographic misorientations.

We have shown that the analysis of rocksalt samples in the SEM using EBSD is a relatively simple process. The samples were prepared in the same manner as for reflected light microscopy analysis (with the addition of some conductive paint to the edges), and images which show the same information as reflected light photomicrographs are easily obtained. An automated EBSD analysis of a 300×300 grid, as used here to study the dry rocksalt sample (Fig. 4c), can take as little as 4 h (depending on the number of phases and their respective crystal systems). Not only does this provide misorientation maps as we have shown, but all the crystallographic orientation data for that area are readily accessible and can be used in whatever manner is desired. For example, pole figures, inverse pole figures, rotation axes and misorientation frequency distributions can easily be calculated and plotted. Such information on internal lattice orientation variations (as shown in Fig. 3) may even be useful in characterising the relative timing of recrystallisation of different

grains in a polycrystalline sample. For example, in a microstructure dominated by grain boundary migration, newly recrystallised grains would generally contain less internal lattice orientation variation than older grains, and it should be possible to identify the presence of separate grains sharing a common orientation—'orientation families' (see Urai et al., 1986). This powerful technique allows us to quantify fully any microstructure and lattice preferred orientation in deformed rocksalt. Recent studies on other minerals using EBSD have demonstrated the possibilities of analysing and interpreting microstructures in this manner (e.g. Trimby, 1998; Trimby et al., 1998; Faul and Fitz Gerald, 1999; Fliervoet et al., 1999). Other potential applications of EBSD to rocksalt include measuring the extent of subgrain rotation with increasing strain, estimating the rate of new grain nucleation, and evaluating the importance of individual slip systems in forming lattice preferred orientations. A full review of the application of EBSD to geological samples is given in Prior et al. (1999).

Despite such developments, the technique still has drawbacks. For example, a superficial look at the central grain in the boundary misorientation map of the wet salt sample (Fig. 2c) would indicate an absence of significant substructure. Further processing of the EBSD data is clearly necessary to identify the presence of any considerable orientation changes across the grain (Fig. 3). Yet it would take a single glance at the etched surface using reflected light microscopy (Fig. 2a) to show that the grain interior contains numerous low angle subgrain boundaries. Another drawback is in the analysis of larger areas ($>1 \times 1$ mm), when it becomes necessary to move the SEM stage instead of the electron beam. With our current set-up, this takes $\sim$0.75 s for each measurement in a rocksalt sample, resulting in an analysis time of $\sim$19 h for a 300×300 grid. It is important, therefore, to use this powerful technique wisely, as a complement to light microscopy, not as a replacement: why take 1 day to collect 90 000 orientation measurements when a single optical image of an etched surface will suffice? For this reason it becomes important to understand the nature of etched boundaries, and the type of boundary that they represent.

It is clear from both the dry and the wet salt samples that the reflected light images of the etched surfaces show many more boundaries than the boundary misorientation maps, i.e. boundaries with misorientations $<2^\circ$ (Figs. 2 and 4). Although it is possible to display more boundaries in a misorientation map by setting the minimum misorientation to 1°, this also introduces a number of 'boundaries' which are artefacts resulting from the angular errors involved in EBSP indexing. We know from the present results that most of the boundaries which are not heavily etched

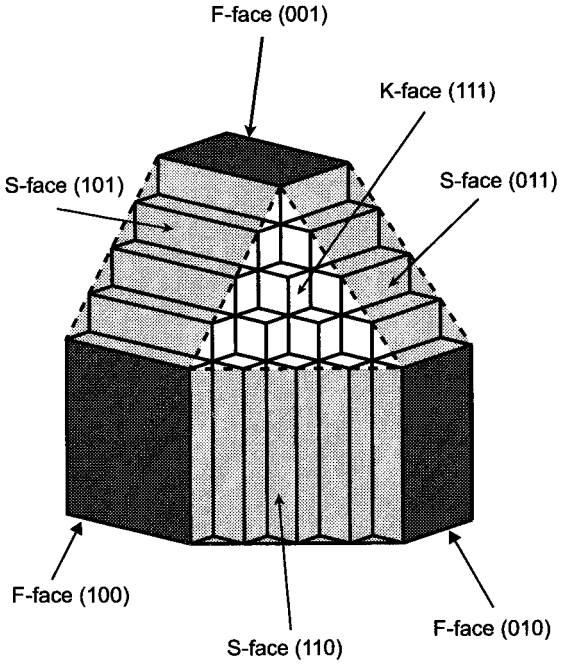

Fig. 7. A schematic diagram showing a hypothetical halite crystal, with the three different types of face: the F-(*flat*-)faces ({100}), the S-(*stepped*-)faces, ({101}) and the K-(*kink*-)faces ({111}). Modified from Hartman (1953).

have misorientations $<2^\circ$, and many of these have misorientations $<1^\circ$ (see Fig. 3). What is more surprising, however, is that many of the intra-granular boundaries which are more heavily etched (see Fig. 4) also have misorientations $<2^\circ$. Interpretations of the dry salt microstructure based solely on the intensity of boundary etching would therefore indicate that subgrain rotation may have progressed to a considerable extent, with many intra-granular boundaries acquiring relatively large misorientations. In general, however, the EBSD data show that this is not true, so caution is needed in interpreting the reflected light images.

In addition, the orientation of the crystal lattice with respect to the sample surface clearly has a substantial effect on the etching (Figs. 5 and 6). Where grains have a {100} face sub-parallel to the sample surface the intensity of etching is low. In contrast grains with a {111} face sub-parallel to the sample surface are strongly etched.

The {100} faces are F-faces (flat faces) which make up the cube form of halite (Fig. 7) (e.g. Hartman, 1953); theoretically such faces are characterised by a shortage of sites for the attachment or detachment of ions. Conversely, the {111} faces are K-faces (kink faces) which are characterised by an abundance of ionic attachment/detachment sites. If an abundance of ionic attachment/detachment sites results in high dissolution rates during etching, then the surface crystallographic orientation has a strong control on the

surface etching rate. The depth of etching at subgrain boundaries is, however, not only controlled by dissolution of the surface but also by the difference in dissolution rate between the boundary itself and the adjacent surface. Dissolution along the boundary will be influenced by its misorientation and, possibly, by the orientation of dislocations within the boundary.

Our results imply that there is a small difference in etching rate between subgrain boundaries and {100} surfaces, but a large relative etching rate between subgrain boundaries and {111} surfaces. The errors involved in calculating the misorientation rotation axes across low angle boundaries preclude an in-depth analysis of potential dislocation types and orientations. With these uncertainties, and without further information about the spatial orientation of the etched low angle boundaries, we cannot be certain as to the exact cause of the variations in etching intensity with different crystallographic orientation. Clearly, though, these variations in the etching intensity should be taken into account when interpreting reflected light photomicrographs.

Geologists can learn a lot about the effect of recrystallisation mechanisms on the rheology and microstructures of deformed rocks by looking at simpler monominerallic systems, such as deformed rocksalt. Imaging the etched surfaces of deformed rocksalt samples can tell us many things about its microstructural characteristics, and it does seem that the depth of etching can be used to distinguish high angle grain boundaries from low angle subgrain boundaries. However, the intensity of etching of subgrain boundaries is influenced more by the host grain's crystallographic orientation than by the boundaries' misorientations. This means that when a more in-depth microstructural investigation is required, the additional data obtained from an EBSD analysis in the SEM are invaluable. We envisage future advances in SEM technology making such fully quantitative studies more common. Nevertheless, etching of rocksalt samples will remain an essential and highly useful part of the initial microstructural analysis.

Acknowledgements

We would like to thank Colin Peach, Wout Pijpers and Pieter van Krieken for carrying out the deformation experiments, and Jaap Liezenberg for preparing the polished and etched samples. The electron microscopy studies were conducted at EMSA, the Utrecht University Centre for Electron Microscopy and Structure Analysis. Pim van Maurik helped with the EBSD–SEM set up, and the EBSD software was supplied by HKL technology, Denmark. The authors benefited from discussions with Cornelis Woensdregt, and thank John Humphreys for use of his V-Map software. Geoff Lloyd, Janos Urai and Cees Passchier are thanked for their helpful reviews and comments. PWT and MRD gratefully acknowledge funding from an NWO-PIONIER subsidy. The rocksalt samples were deformed in the framework of a project on salt rheology (CJS) funded by Shell (Houston).

References

Adams, B.L., Wright, S.I., Kunze, K., 1993. Orientation imaging: the emergence of a new microscopy. Metallurgical Transactions A 24A, 819–831.

Carter, N.L., Hansen, F.D., 1983. Creep of rocksalt. Tectonophysics 92, 275–333.

Carter, N.L., Horseman, S.T., Russell, J.E., Handin, J., 1993. Rheology of rocksalt. Journal of Structural Geology 15, 1257–1271.

Dingley, D.J., Randle, V., 1992. Microstructure determination by electron back-scatter diffraction. Journal of Materials Science 27, 4545–4566.

Dingley, D.J., 1984. Diffraction from sub-micron areas using electron backscattering in a scanning electron microscope. Scanning Electron Microscopy 1984-II, 569–575.

Drury, M.R., Urai, J.L., 1990. Deformation-related recrystallization processes. Tectonophysics 172, 235–253.

Duval, B., Cramez, C., Jackson, M.P.A., 1992. Raft tectonics in the Kwanza Basin, Angola. Marine and Petroleum Geology 9, 389–404.

Faul, U.H., Fitz Gerald, J.D., 1999. Grain misorientations in partially molten olivine aggregates: an electron backscatter diffraction study. Physics and Chemistry of Minerals 26, 187–197.

Field, D.P., 1995. Quantification of partly recrystallized polycrystals using electron backscatter diffraction. Materials Science and Engineering A 190, 241–246.

Field, D.P., 1997. Recent advances in the application of orientation imaging. Ultramicroscopy 67, 1–9.

Fliervoet, T.F., Drury, M.R., Chopra, P.N., 1999. Crystallographic preferred orientations and misorientations in some olivine rocks deformed by diffusion or dislocation creep. Tectonophysics 303, 1–27.

Friedman, M., Dula, W.F., Gangi, A.F., Gazonas, G.A., 1984. Structural petrology of experimentally deformed synthetic rocksalt. In: Hardy Jr., H.R., Langer, M. (Eds.), The Mechanical Behavior of Salt—Proceedings of the First Conference. Trans Tech Publications, Germany, pp. 19–36.

Goyal, A., Specht, E.D., Wang, Z.L., Kroeger, D.M., 1997. Grain boundary studies of high-temperature superconducting materials using electron backscatter Kikuchi diffraction. Ultramicroscopy 67, 35–57.

Guillopé, M., Poirier, J.P., 1979. Dynamic recrystallization during creep of single-crystalline halite: an experimental study. Journal of Geophysical Research 84, 5557–5567.

Hartman, P., 1953. Relations between structure and morphology of crystals. PhD thesis, Rijksuniversiteit te Groningen.

Heard, H.C., 1972. Steady state flow in polycrystalline halite at a pressure of two kilobars. In: Heard, H.C., Borg, I.Y., Carter, N.L., Raleigh, C.B. (Eds.), Flow and Fracture of Rocks. American Geophysical Union Geophysical Monograph 16, pp. 191–209.

Janssen, L.G.J., Prij, J., Kevenaar, J.W.A.M., Jong, C.J.T., Klok, J., Beemsterboer, C., 1984. The thermo-mechanical behaviour of a salt dome with a heat generating waste repository. European

Communities Commission, Nuclear Science and Technology Series, EUR-9205.

Mendelson, S., 1961. Dislocation etch formation in sodium chloride. Journal of Applied Physics 32, 1579–1582.

Peach, C.J., 1991. Influence of deformation on the fluid transport properties of salt rocks. Geologica Ultraiectina 77. PhD thesis, Utrecht University.

Peach, C.J., Spiers, C.J., 1996. Influence of plastic deformation on dilatancy and permeability development in synthetic salt rock. Tectonophysics 256, 101–128.

Prior, D.J., Trimby, P.W., Weber, U.D., Dingley, D.J., 1996. Orientation contrast imaging of microstructures in rocks using forescatter detectors in the scanning electron microscope. Mineralogical Magazine 60, 859–869.

Prior, D.J., Boyle, A.P., Brenker, F., Cheadle, M.C., Day, A., Lopez, G., Potts, G.J., Reddy, S., Speiss, R., Timms, N.E., Trimby, P.W., Wheeler, J., Zetterström, L., 1999. The application of electron backscatter diffraction and orientation contrast imaging in the SEM to textural problems in rocks. American Mineralogist (in press).

Randle, V., 1992. Microtexture Determination and its Applications. The Institute of Materials, London.

Randle, V., 1993. The measurement of grain boundary geometry. Electron Microscopy in Materials Science Series, Institute of Physics Publishing, Bristol.

Senseny, P.E., Hansen, F.D., Russel, J.E., Carter, N.L., Handin, J.W., 1992. Mechanical behaviour of rocksalt: phenomenology and micromechanisms. International Journal of Rock Mechanics, Mining Sciences and Geomechanics Abstracts 29 (4), 363–378.

Spiers, C.J., Urai, J.L., Lister, G.S., Boland, J.N., Zwart, H.J., 1986. The influence of fluid–rock interaction on the rheology of salt rock. European Communities Commission, Nuclear Science and Technology Series, EUR-10399.

Spiers, C.J., Peach, C.J., Brezowsky, R.H., Schutjens, P.M.T.M., Liezenberg, J.L., Zwart, H.J., 1989. Long-term rheological and transport properties of dry and wet salt rocks. European Communities Commission, Nuclear Science and Technology Series, EUR-11848.

Spiers, C.J., Schutjens, P.M.T.M., Brezowsky, R.H., Peach, C.J., Liezenberg, J.L., Zwart, H.J., 1990. Experimental determination of constitutive parameters governing creep of rocksalt by pressure solution. In: Knipe, R.J., Rutter, E.H. (Eds.), Deformation Mechanisms, Rheology and Tectonics, Geological Society Special Publication 54, pp. 215–227.

Spiers, C.J., Carter, N.L., 1998. Microphysics of rocksalt flow in nature. In: Aubertin, M., Hardy Jr., H.R. (Eds.), The Mechanical Behavior of Salt IV—Proceedings of the Fourth Conference. Trans Tech Publications, Germany, pp. 115–128.

Sutherland, H.J., Cave, S.P., 1980. Argon gas permeability of New Mexico rock salt under hydrostatic compression. International Journal of Rock Mechanics, Mining Sciences and Geomechanics Abstracts 17, 281–288.

Trimby, P.W., Prior, D.J., Wheeler, J., 1998. Grain boundary hierarchy development in a quartz mylonite. Journal of Structural Geology 20, 917–935.

Trimby, P.W., Prior, D.J., 1999. Microstructural imaging techniques—a comparison between light and scanning electron microscopy. Tectonophysics 303, 71–81.

Trimby, P.W., 1998. Quantifying microstructures—the development and application of a new technique to quartzitic shear zones. PhD thesis, University of Liverpool.

Urai, J.L., Means, W.D., Lister, G.S., 1986. Dynamic recrystallization of minerals. In: Hobbs, B.E., Heard, H.C. (Eds.), Mineral and Rock Deformation: Laboratory Studies—The Paterson Volume. American Geophysical Union Geophysical Monograph 36, pp. 161–199.

Urai, J.L., Spiers, C.J., Peach, C.J., Franssen, R.C.M.W., Liezenberg, J.L., 1987. Deformation mechanisms operating in naturally deformed halite rocks as deduced from microstructural investigations. Geologie en Mijnbouw 66, 165–176.

Venables, J.A., Harland, C.J., 1972. Electron back-scattering patterns—a new technique for obtaining crystallographic information in the scanning electron microscope. Philosophical Magazine 27, 1193–1200.

Wawersik, W.R., Zeuch, D.H., 1986. Modelling and mechanistic interpretation of creep of rocksalt below 200°C. Tectonophysics 121, 125–152.

Weijermans, R., Jackson, M.P.A., Venderville, B., 1993. Rheological and tectonic modelling of salt provinces. Tectonophysics 217, 143–174.

Wenk, H.R., Canova, G.R., Molinari, A., Mecking, H., 1989. Texture development in halite: comparison of Taylor model and self-consistent theory. Acta Metallurgica 37, 2017–2029.

Wenk, H.R., Canova, G.R., Bréchet, Y., Flandin, L., 1997. A deformation-based model for recrystallization of anisotropic materials. Acta Materialia 45, 3283–3296.